Investigation of the tip-leakage losses in turbine axial stages

A Szymański, S Dykas, W Wróblewski and S Rulik
Institute of Power Engineering and Turbomachinery, Silesian University of Technology, 44-100 Gliwice, ul. Konarskiego 18, Poland

E-mail: artur.szymanski@polsl.pl

Abstract. In turbomachinery, an influence of a tip-leakage flow on overall blade loss is crucial and its reduction is still worth striving for. In this paper a numerical analysis of the flow in tip seal of high-rotating gas turbine engine has been made. This analysis is a part of experimental research for testing the commercially used different tip seals solutions. Described test rig is predicted to be an universal tool for developing and examining different configurations of turbine blade tips. Presented numerical analysis is used to predict physical phenomena that may affect the rotor blade performance. In the numerical investigation the commercial Ansys CFX software was employed. The most important parameters were: mass flow rate at the inlet and outlet of the test bench, pressure and velocity distribution and the air temperature growth above the rotor. Also, an influence of test rig inlet and outlet geometry on flow uniformity was investigated. During the analysis the attention was focused also on minimizing the turbulence intensity in outlet area, that could cause significant difficulties in flow and stable work of the machine – generated eddies contributes to lower the mass flow rate.

1. Introduction

In gas turbines applied the leakage flow has a crucial impact on the efficiency. Seals isolate a region of a higher pressure from one of a lower pressure when relative rotational motion occurs, to prevent the leakage. There are many types of seals, for instance gas annular seals reduce leakage well, but it takes certain amount of air from compressor, reducing performance of entire machine. Although new designs of film riding and contacting seals that fundamentally reduce leakage [1, 2], the labyrinth seal constantly is a prime turbine sealing solution because of low price, low maintenance, minimal rub particulate contamination and high temperature capability. However, operating at tight clearances and high pressure ratios, tend to develop considerable force imbalance and dynamic phenomenon, like rotor vibrations. Honeycomb seals were first applied in 1989 in High Pressure Oxygen Turbo Pump in Space Shuttle main engine [3]. Application of honeycomb seals improves rotordynamic performance and force balance, reducing vibrations provides high resistance to flow in peripheral as well as axial directions. Works found in literature give weight the importance of friction factor coefficient evaluation for anticipation of the seal rotor-dynamic characteristics. Majority of researches, both experimental and computational, have focused their attention on stationary configurations – where the relative motion of rotor and stator has been omitted. Stationary test-rigs are much more workable than rotational ones, but an overlooking of a rotational velocity component may affect the test results significantly. Experimental and theoretical predictions on seal configuration performed by Childs and Kleynhans [4], found six parameters influencing rotor dynamics coefficients – associated with friction factor: seal inlet pressure, pressure ratio across the seal, seal clearance, seal inlet fluid rotation, rotor speed and honeycomb cell width. Experimental analysis performed on static set rig by Al-Qutub et al.

Content from this work may be used under the terms of the Creative Commons Attribution 3.0 licence. Any further distribution of this work must maintain attribution to the author(s) and the title of the work, journal citation and DOI.
Published under licence by IOP Publishing Ltd

[5], found out a dependency on friction factor on clearance and Reynolds number only. Rotational test rigs give full outlook on the phenomena which occur in actual sealing. Results from preliminary CFD calculations are presented in this paper. In the first section test rig and used CFD model is described. This is followed by review of used non-dimensional parameters to describe results. Finally, conclusions and future work ideas are given.

2. Description of designed test rig

Numerical campaign exploiting steady state RANS analysis has been performed to support the design process of the test facility. Presented test rig setup consists of Roots type vacuum pump with a capacity of 600 m^3/h connected directly to the pressure tank of 3 m^3 volume. Tank is connected to the test rig by a pipeline. The valve between the rig and the pressure tank allows to adjust the pressure at outlet. A scheme of the installation is shown in Figure 1.

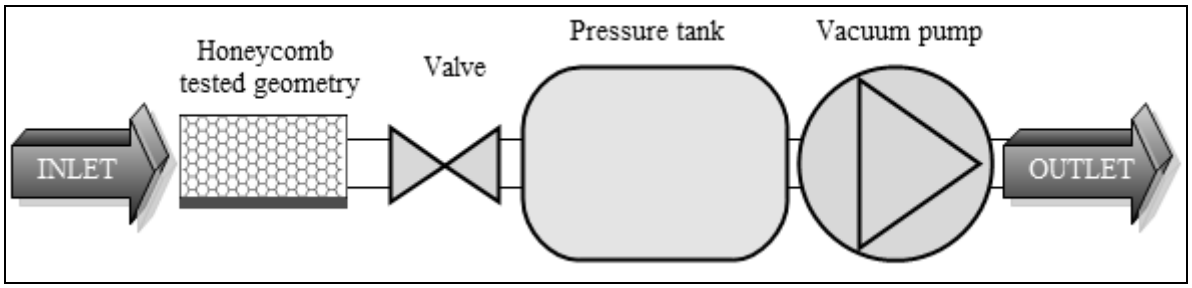


Figure 1. Test rig scheme

Described test rig was designed to investigate various types of sealing system, but mostly "honeycomb on labyrinth" or "smooth on labyrinth". Due to its construction, the test rig allows to inquire different types of sealing, by a large variety of inlet and outlet geometry configurations. Iconic parameters of rotational test bench are gathered in Table 1. This work shows CFD calculation for "smooth on labyrinth" case. Aims of analysis are to check impact of rotor surface roughness, and rotational velocity both on mass flow rate through the labyrinth seal and velocity components. Results are believed to support designing decisions.

Table 1. Parameters of designed test rig.

Maximum mass flow rate (air)	0.2 kg/s
Pressure ratio, up to	0.5
Rotational speed, up to	24000 rpm
Seal outer diameter (rotor), up to	290 mm
Working temperature	Ambient

3. CFD model

In this article a stationary analysis of flow through sealing system "labyrinth on smooth" has been done. For CFD calculations commercial software Ansys CFX has been used. Investigated labyrinth sealing consists of two oblique fins, and is typical in gas turbines appliances. In this case radial dimension of cavity is 0.5 mm, and length (at top) of one fin is 1.45 mm. Analyzed geometry is shown in Figure 2.

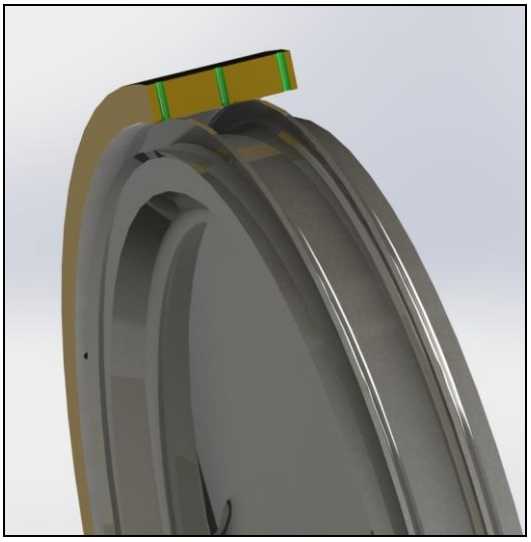


Figure 2. Geometry of described labyrinth seal test rig.

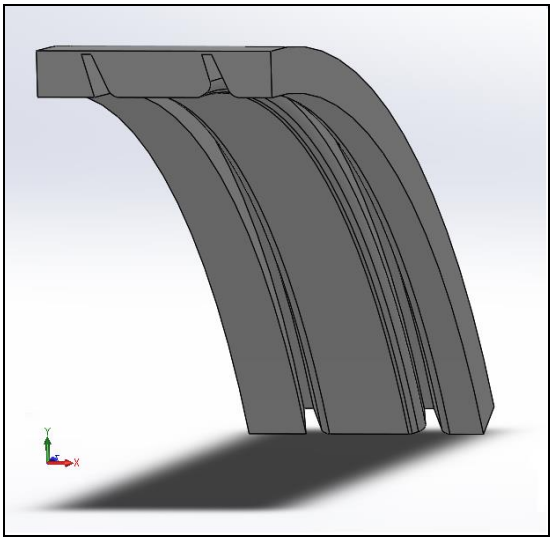


Figure 3. Geometry of 60° fluid above rotor.

For discretization the volume of flow in rotor a structural mesh has been used. To obtain both good mesh quality and low time of calculations a 60° geometry has been generated. This procedure let us minimalize number of mesh elements, while accuracy of calculations remains high. The geometry of fluid above the seal is shown in Figure 3. The mesh of rotor – area above the labyrinth seal consists of 2.6M nodes. The mesh was done with good wall layers discretization – parameter $y^+ \approx 1$. Described mesh is presented in Figure 4.

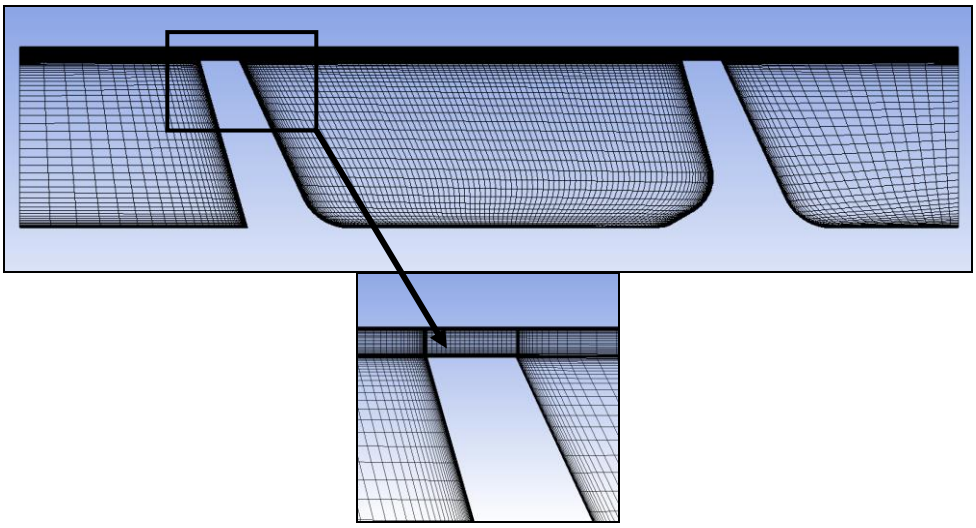


Figure 4. Structural mesh of the rotor domain.

Reference analysis was performed with stationary domain of rotor, in the rest of cases rotational speed varies. Moreover, the in reference case walls of rotor and stator were assumed as smooth, in the rest of cases rotor roughness varies. In each case walls were adiabatic. At sides of rotor – perpendicular to inlet and outlet, a rotational periodicity interface was chosen. Convergence criteria were set to 10^{-5} of RMS, with mass imbalance at rotor domain under 0.1%. Both advection scheme and turbulence numeric were set to high resolution. Boundary conditions are presented in Tab. 2.

Table 2. Boundary conditions used in CFX model

GLOBAL	Turbulence model	SST
	Gas model	Air ideal gas
	Heat transfer	Total energy
	Viscous work term	Yes
	Reference pressure	0 bar
	Timescale	Local
INLET	Total pressure	1 bar
	Total temperature	293 K
	Turbulence intensively	5 %
OUTLET	Total pressure	0.9 bar
	Pressure averaging	Yes

4. CFD results

Results are presented as dimensionless values. Relative mass flow rate was calculated as m_{RPM}/m_{RPM0}, where m_{RPM} – is mass flow rate for given *RPM* , m_{RPM0} – mass flow rate for reference case (i.e. for 0 *RPM*). In each case relative mass flow rate was shown as a function of circumferential rotor velocity, to axial-flow velocity – u/c_{ax}. An arrow depicted in Figure 5 shows plane where the data for further calculation are taken from. Axial-flow velocity is calculated as mass flow averaged velocity X component, in rotational cases as velocity in stationary frame X component.

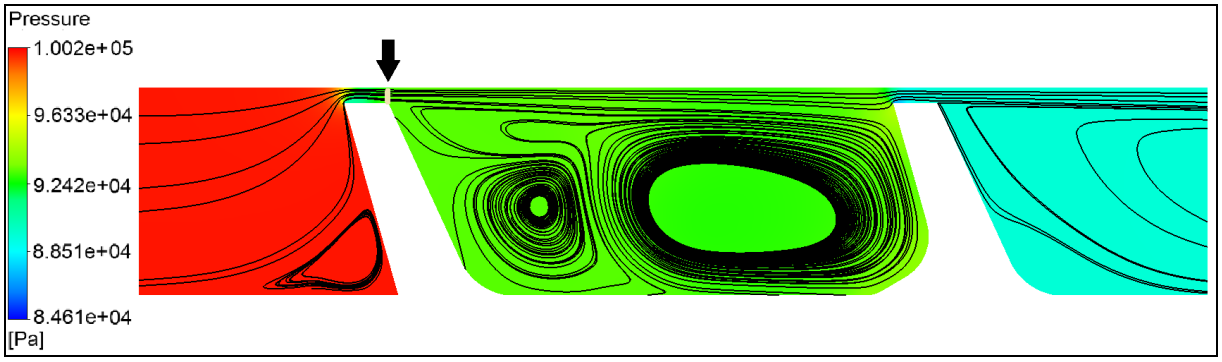


Figure 5. Streamlines superimposed on contours of static pressure for reference, smooth walls, non-rotating case.

4.1. Results of rotational speed influence on relative mass flow rate

In this case only efect of rotational speed on mass flow rate was inqired. Rotor walls were set as smooth. For described geometry certain influence was found. Relative mass flow was described as m_{RPM}/m_{0RPM}, where m_{RPM} – is mass flow for various rotational velocity, and m_{0RPM} is result for stationary case. Relative mass flow decreases in function of rotational speed. The lowest mass flow coresponds to the highest rotational speed. The dependecy is shown in Figure 6. Due to limitation of roational speed – 24000 *RPM* – of the test rig, maximum u/c_{ax} is ca 4. This value corrsponds to relative mass flow rate at 0.88.

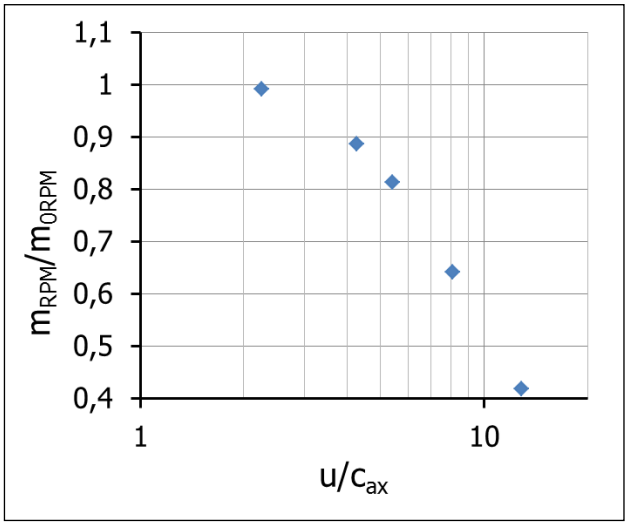


Figure 6. Rotational speed impact on discharge characteristic.

4.2. Results of surface roughness influence on relative mass flow rate

Default wall roughness in CFX is set to smooth – it means that wall condition has no influence on flow. In actual devices roughness has crucial impact both on flow and construction parameters. Roughness is considered to be determinant of part performance. As a consequence, constructors establish an upper limit on roughness. In this work three different values of roughness were set on rotating wall – sedentary wall remain smooth to investigate influence only the rotor roughness. This analysis was done to establish lower limit of surface roughness – to minimalize mass flow through the seal. Values of roughness corresponding to different types of material finishing, are presented in Table 3.

Table 3. Examined values of roughness.

Type of material finishing	**Roughness value**
Fine machining/grinding	2.5 μm
Thorough machining	10 μm
Coarse machining	50 μm

Results of roughness influence investigation are shown in the Fig. 7. Relative mass flow was described as $m_{RPM,Ra}/m_{0RPM,Ra}$, where $m_{RPM,Ra}$ – is mass flow for various rotational velocity and the same surface roughness, and $m_{0RPM,Ra}$ is result for stationary case with the same roughness as rotational case. For higher values of relative circumferential velocity, impact of surface roughness is stronger. The highest value of roughness Ra = 50 μm corresponds with rapid drop of mass flow rate. The difference in relative mass flow rate between for highest rotational velocity and reference case is 20.1 %, which means that mass flow rate, and axial velocity drops, while u/c_{ax} rises. In table 4 the values of relative mass flow for different rotational velocities and surface roughness are shown. For higher velocities, the difference between smooth and rough wall is significant, and is equal to 8 % in smooth vs. 50 μm case for 24000 rpm. This proves that roughness has strong influence on flow regime in seal, and to reduce leakage should be as high as possible. Also another conclusion can be made, that roughness shouldn't be omitted in CFD analysis.

Table 4. Rotational speed and surface roughness dependency on rel. mass flow

	50 µm	**10 µm**	**2.5 µm**	**Smooth**
Rotational velocity (rpm)	**m/m_0**	**m/m_0**	**m/m_0**	**m/m_0**
0	1	1	1	1
7500	1	1	1	1
15000	0.959	0.983	0.987	0.991
20000	0.887	0.927	0.939	0.942
24000	0.799	0.864	0.877	0.882

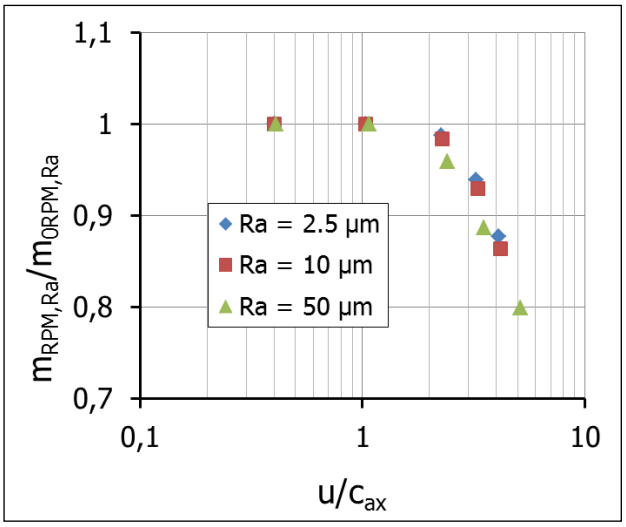


Figure 7. Roughness and rotational speed imact on relative mass flow.

4.3 Results of inlet angle influence on relative mass flow rate

Default angle of inlet flow in CFX is set to 90°. Mentioned angle is measured between inlet velocity direction and circumferential direction, as shown in Figure 8.

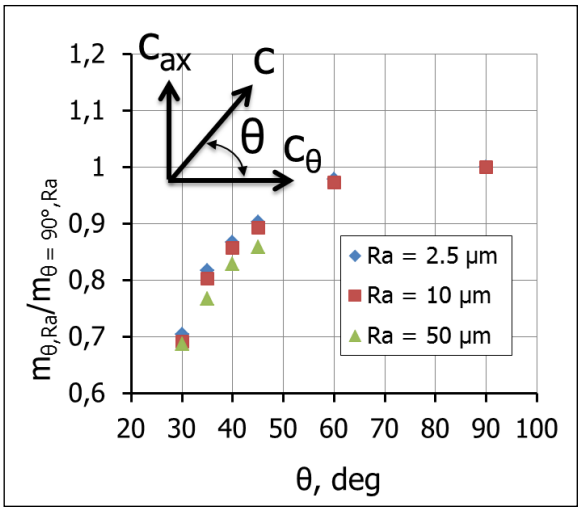


Figure 8. Impact of inlet velocity angle on discharge characteristic for 20000 rpm.

Results of roughness inlet velocity investigation are shown in the Fig. 8. Relative mass flow was described as $m_\theta/m_{\theta = 90°}$, where m_θ – is mass flow for various inlet velocity angle the same surface roughness as reference value, and $m_{\theta = 90°}$ is result for reference case with flow angle 90°. Every point was calculated for the same rotational velocity 20000 rpm. Both for high values of θ angle – 60° and low – 30° impact of surface roughness was slight. For mentioned angles difference of relative mass flow rate between 2.5 μm and 50 μm roughness case is up to 1.5 percent points. The highest difference was observed for inlet angles 35° – 45°, and was equal up to 5 %. This proves that inlet velocity angle has strong influence on flow regime in seal, and to reduce leakage should be as high as possible. Also another conclusion can be made, that roughness has the highest impact for inlet velocity angles ca. 45°.

5. Conclusions and future work

Numerical calculations were performed and analyzed for the impact both of rotational speed and surface roughness on the discharge characteristics of labyrinth seal geometry. The CFD analysis confirmed that onset of drop in mass flow through the leakage depends on critical value of characteristic velocity, $u/c_{ax} = 1$ – as reported previously by Waschka [2]. For designed geometry influence of rotational velocity up to 24000 rpm on relative mass flow rate was up to 12% reduction, in case with smooth walls. When wall roughness is considered, relative mass flow rate drops by 20,1 % - for maximum rotational velocity and roughness. This work provided information, that surface roughness can be very important aspect in designing labyrinth seals. Also seal inlet fluid rotation has an impact on seal discharge. For presented geometry rel. mass flow rate drops 31% for case with roughness 50 μm and inlet angle 30°. Although, roughness has strong influence only for exact range of inlet angle values. For extreme values of this angle (namely – lower than 30° and higher than 60°), its influence was slight. It shows, that for the presented seal geometry, there is strong possibility to improve its work by simply modifying surface roughness and applying pre-swirl nozzles at inlet.
The future work will cover the more expanded CFD calculations, including transient – time dependent models, comparison presented results with both other turbulence models and different boundary conditions – pressure ratios (to get higher flow velocity and Reynolds numbers), flow pre-swirl on inlet for higher rotational velocities and surface roughness. Another task is compare results and finally validation presented data with experiment done on rotational and stationary test rigs.

6. References

[1] Paolillo R 2006 Rotating Seal Rig Experiments: Test Results and Analysis Modeling, *ASME Turbo Expo 2006: Power for Land, Sea and Air* **3** pp 1551-1559
[2] Waschka W 1992 Influence of high rotational speeds on the heat transfer and discharge coefficients in labyrinth seals, *ASME Paper 90-GT-330 Journal of Turbomachinery* **114** pp 462-468
[3] Scharrer J 1989 Discussion in paper, annular honeycomb seals: test results for leakage and rotordynamic coefficients; comparisons to labyrinth and smooth configurations. *ASME J. Tribol*. **111** pp 300-301
[4] Childs D W and Kleynhans G F 1992 Experimental rotordynamic and leakage results for short (l/d) honeycomb and smooth annular pressure seals. *IMechE Proceedings, Fifth international Conference on Vibrations in Rotating Machinery* **11** pp 305-311
[5] Al-Qutub A M, Elrod D and Coleman H W 2000 A new friction factor model and entrance loss coefficient for honeycomb annular gas seals. *ASME J Tribol 200*;**122** pp 622-627



https://dspace.org/

Investigation of the tip-leakage losses in turbine axial stages

Szymaski, Artur; Dykas, S.; Wróblewski, W.; Rulik, S.

2014-12
Institute of Physics (IOP)
http://dx.doi.org/10.1088/1742-6596/530/1/012033
A Szymaski, S Dykas, W Wróblewski and S Rulik. Investigation of the tip-leakage losses in turbine axial stages. Journal of Physics: Conference Series, Vol. 530, Conference 1, article number 012033

Downloaded from a DSpace repository. https://dspace.org/